

Sotol bagasse (*Dasyliirion* sp.) as a novel feedstock to produce bioethanol 2G: Bioprocess design and biomass characterization

Jésica de Jesús González-Chavez^a, Christian Arenas-Grimaldo^a, Lorena Amaya-Delgado^b, Edgar Vázquez-Núñez^a, Santiago Suarez-Vázquez^c, Arquímedes Cruz-López^c, Juan Gabriel Segovia-Hernández^d, Samuel Pérez-Vega^e, Iván Salmerón^e, Carlos E. Molina-Guerrero^{a,*},¹

^a Universidad de Guanajuato, Departamento de Ingenierías Química, Electrónica y Biomédica, División de Ciencias e Ingenierías, Campus León, Lomas del Bosque 103, Col. Lomas del Campestre, León C.P. 37150, Guanajuato, Mexico

^b Centro de Investigación y Asistencia Tecnológica del Estado de Jalisco, Av. de los Normalistas 800, Colinas de La Normal, Guadalajara C.P. 44270, Jalisco, Mexico

^c Universidad Autónoma de Nuevo León, Facultad de Ingeniería Civil, Departamento de Ingeniería Ambiental, Av. Universidad S/N, Ciudad Universitaria, San Nicolás de los Garza C.P. 66455, Nuevo León, Mexico

^d Universidad de Guanajuato, Departamento de Ingeniería Química, División de Ciencias Naturales y Exactas, Noria Alta s/n, Col. Noria Alta, Guanajuato C.P. 36000, Guanajuato, Mexico

^e Universidad Autónoma de Chihuahua, Facultad de Ciencias Químicas, Circuito 1, Nuevo Campus Universitario, Chihuahua C.P. 31125, Chihuahua, Mexico

ARTICLE INFO

Keywords:

Circular bioeconomy
Kluyveromyces marxianus
Renewable energy

ABSTRACT

Sotol (*Dasyliirion* spp.) is a plant endemic to northern Mexico used since ancient times by North American Indians. In the present research, we studied the transformation of lignocellulosic Sotol Bagasse (SB) components as a feedstock for bioethanol 2G production. For this purpose, SB was pretreated with diluted acid (AP) and alkali (BP). In AP, biomass was exposed to different acid concentrations and reactions proceeded at different times according to a 3² experimental design. BP was performed by stirring SB with a 3 M NaOH solution at 30 °C and 120 rpm for 6 h. Pretreated samples were hydrolyzed using the Cellic CTec2® enzyme complex. These experiments were performed at the micro-level. Two conditions presented the best performance: AP1 (0.5% v/v acid; 15 min; 121 °C) and AP2 (1% v/v acid; 30 min; 121 °C). Then, AP1 and AP2 were selected for process scale-up, resulting in RS yields of 22.4% and 19.46%, respectively. The sugars produced were fermented in presence of *Kluyveromyces marxianus* producing an 81.85% ethanol yield. Data indicated that fermentation of SB treated with AP1 produced ethanol. In addition, fermentation of SB pretreated with AP2 generated ethanol and low concentrations of iso-butanol, acetaldehyde, and isoamyl alcohol. Ethanol and energy yield of AP1 treated biomass were 0.19 L bioethanol and 4.09 MJ per kg SB. These results proved that the proposed process is sustainable and can potentially be used for bioethanol 2G production using SB. As a result, circular bioeconomy will be stimulated.

1. Introduction

Sotol (*Dasyliirion* sp.) is a plant that belongs to the *Nolinaceae* family. This plant, endemic to the Chihuahuan desert, is found in northern Mexico (Chihuahua, Coahuila, Durango, and Zacatecas) and southern United States (Texas and New Mexico), where extreme climate prevails (Zavala-Díaz de la Serna et al., 2020). Flores-Gallegos et al. (2019) reported that this plant has been used since ancient times for ornamental

and building purposes, among others. Moreover, in the pre-Hispanic period, North American Indians used to drink fermented sotol. More recently, a liquor called sotol or sereque was obtained after a distillation process (Flores-Gallegos et al., 2019). Despite the fact that sotol displays different nutritional properties, for many years industry remained uninterested in this product (Bell and Castetter, 1941). However, in recent times, this fermented beverage (sotol) has received a designation of origin. For this reason, a regulation has been promulgated in the states of

* Corresponding author.

E-mail address: ce.molina@ugto.mx (C.E. Molina-Guerrero).

¹ ORCID: 0000-0001-5992-0379.

Chihuahua, Coahuila, and Durango (Official Mexican Standard NOM-159-SCFI, 2004), promoting sotal industrialization and production.

Similar to tequila, during sotal production the plant pineapple is cooked. The resulting liquid that contains extracted sugars is fermented and distilled (Flores-Gallegos et al., 2019). Different publications have described the microbial communities responsible for sotal fermentation (Zavala-Díaz de la Serna et al., 2020). During sugars extraction, a lignocellulosic residue called sotal bagasse (SB) is obtained. As it was reported in Flores-Gallegos et al. (2019), sotal industry generates a lot of waste, which is used for animal feed, in the best case. It has been reported that sotal production has increased. However, no precise data are available on the amount of residues generated by this industry. Inadequate disposal of this agro-industrial wastes (AIW) results in negative environmental impacts. In Mexico, AIW management has not been regulated. For this reason, environmental pollution caused by improper AIW disposal is a common problem in this country (Carrillo-Nieves et al., 2019).

Several researchers have reported the energy potential of different biomasses. They include wheat and corn straw, sugarcane bagasse, bean stubble, and coffee waste, among others (Carrillo-Nieves et al., 2019; Molina-Guerrero et al., 2020). Specifically, lignocellulosic biomass feedstocks (LBF) are considered potential energy sources in the process of transitioning from a petroleum-based economy to a bioeconomy (Bajwa et al., 2018; Ighathinathane and Sanderson, 2018).

AIW biomass represents one of the renewable resources essential in the development of bioeconomy (Manzanares, 2020). The bioeconomy concept has been defined by the US Department of Energy as “the global industry transition of sustainably utilizing renewable aquatic and terrestrial biomass resources in energy, intermediate and final product for economy, environmental, social, and national security benefits” (US Department of Energy). Bioeconomy can be supported through the generation of biorefineries. In a biorefinery, the biomass or food waste is transformed into fuels or commodity chemicals using chemical and biological strategies (Carrillo-Nieves et al., 2019; Esposito and Antonietti, 2015; Merediane Kochevka et al., 2020). The word biorefinery is derived from oil refinery, where the latter refers to the separation of crude oil into petroleum products, and the former deals with biomass separation (Nagappan and Nakkeeran, 2020). Biomass is able to provide energy and mitigate global warming by consuming carbon dioxide. Biorefinery of biomass involves the use of a wide array of techniques and generation of different valuable products. For example, lignocellulosic materials can be transformed using a conventional biochemical route that is based on four main stages: i) biomass conditioning (grinding, particle size selection, and different pretreatments including acidic, alkaline, and hydrothermal, among others); ii) enzymatic hydrolysis (using a wide variety of enzymes); iii) fermentation (yeast, bacteria); and iv) downstream processes (Nagappan and Nakkeeran, 2020).

Pretreatment is a key stage for AIW transformation. The lignin-carbohydrate composite present in the AIW represents a physical and chemical barrier for the biocatalyst. For this reason, a depolymerization step is required. This process facilitates the access of the biocatalyst to plant polysaccharides to produce fermentable sugars (Luciano Silveira et al., 2015). Currently, different pretreatment processes have been proposed for the transformation of biomass to ethanol. They include the use of alkali, dilute acid, and ionic liquids at relatively low temperatures (121 °C), and autohydrolysis using temperatures between 150 °C and 190 °C (Aguirre-Fierro et al., 2020; Ibrahim et al., 2011; Morais et al., 2016). Subsequently, sugars are transformed into bioethanol or bio-based, high-value-added products through fermentation (Luciano Silveira et al., 2015; Merediane Kochevka et al., 2020).

In the present research, we proposed to use sotal bagasse as a novel carbon source to produce valuable products including second-generation bioethanol (2G). Bioethanol 2G, which can be produced from SB, has been proposed as one of the most promising biofuels that can reduce the dependence on fossil fuels (López-Ortega et al., 2021).

Bioethanol is an oxygenated fuel that contains 35% oxygen. For this reason, particulates and nitrogen oxides (NOx) emissions are reduced during bioethanol combustion (López-Ortega et al., 2021). The world production of bioethanol reached 115 billion L in 2019, amount that represents about 7.7% of the global gasoline demand (Morales et al., 2021). López-Ortega et al. (2021) estimated a potential demand of 3 billion L per year of bioethanol in Mexico. Substitution of gasoline by this amount of bioethanol may result in: i) significant reduction in greenhouse gas emissions; ii) positive impact in national energy security; and iii) increase in business opportunities that promote economic growth (López-Ortega et al., 2021).

Currently, different AIW are under investigation to determine the best conditions to improve ethanol production. It is important to notice that different substrates may require different operative conditions (Sanchez et al., 2013). It has been demonstrated that during the pre-treatment stages, different inhibitory agents may be produced. They include furfural and hydroxymethyl furfural (HMF) that inhibit the growth of microorganisms. For example, it has been reported that inhibition of *Kluyveromyces marxianus* resulted in the generation of different by-products including isobutanol, acetaldehyde, amyl alcohols, among others (Flores-Cosío et al., 2018). The ascomycetous yeast *K. marxianus*, which showed promising results in the production of cellulosic ethanol and renewable chemical compounds (Leonel et al., 2021), has been isolated from traditional fermented dairy products including fermented milk, kefir, yoghurt, and cheese, among others (Karim et al., 2020). This yeast displays high growth rate, is thermotolerant, assimilates toxic compounds, and has a highly resistant cell membrane (Sandoval-Núñez et al., 2017).

The design of process plants (Biorefineries) for the transformation of AIW into bioethanol and subproducts is a topic of ongoing interest (Moncada et al., 2016). Different research groups have reported the designs of plants for the processing of wheat straw, sugarcane bagasse, and apple pomace, among others (López-Ortega et al., 2021; Molina Guerrero et al., 2021; Sanchez et al., 2013). Also, the comparison between different technologies has been published (López-Ortega et al., 2021). Several authors have proposed process designs for biofuels production that include biomass processing and downstream. According to their results, the designs displayed high performances (Oseguera et al., 2018; Torres-Ortega et al., 2018).

In the present research, we performed a micro-reaction, scaling-up (1 L), large scale mass and energy balance, and sotal bagasse (SB) biomass characterization. The objective of this research was to explore and determine the potential use of SB as a feedstock for bioethanol 2G production. The biomass was characterized using X ray diffraction, X ray fluorescence, Total Attenuated Reflection (ATR), and Scanning Electronic Microscopy (SEM). The reaction broth was analyzed by gas chromatography and high-performance liquid chromatography (HPLC). In addition, the calculation of large-scale reactors (mass and energy balance) for the fundamental stages (pretreatment, hydrolysis, and fermentation) was performed. To the best of our knowledge, this is the first report on the use of SB in biotechnological processes.

2. Materials and methods

2.1. Sotal bagasse composition

Sotal bagasse (SB) (*Dasyliion* sp.) was provided by local producers in Chihuahua, Mexico. The composition of structural fibers before and after pretreatment was determined using the AOAC 2012 method (Determination of structural carbohydrates and lignin). Specifically, the content of cellulose, hemicellulose, and lignin were obtained (Sluiter et al., 2011). Analysis was performed at the Center for Biological and Agricultural Sciences (CUCBA), Universidad de Guadalajara.

2.2. Chemical reagents and chemical pretreatments

The chemical reagents used in the present investigation included: (a) Cellic CTec2 (Cellulase, enzyme blend- Hydrolysis > 1000 units/gram) (Sigma-Aldrich) (The cellulase activity was calculated according to (Adney and Baker, 2008) which resulted in enzymatic activity of 201 FPU/mL); Yeast Extract (Sigma-Aldrich); Sodium phosphate dibasic $\geq 99.0\%$ (Sigma-Aldrich); Magnesium phosphate dibasic trihydrate (Bio-Ultra) $\geq 98.0\%$ (KT), D-(+)-Glucose > 99.5%. 99.0% NaOH (J.T. Barker); 1 N H₂SO₄ (Hycel).

SB fibers were subjected to two different chemical pretreatments: (a) alkali; and (b) a diluted sulfuric acid pretreatment. In the alkali pretreatment, SB was exposed to an alkali solution (3 M) at 30 °C with continuous magnetic stirring (120 rpm) for 6 h. Later, the biomass was filtered, neutralized, dried, and stored for further experiments as indicated in Molina et al. (2014). In the acid pretreatment, three reaction times (x (min): 15; 30; 60) and acid concentrations (y (H₂SO₄% v/v): 0.25; 0.5; 1.0) were selected to identify the best pretreatment conditions. The tests were carried out according to a 3² factorial design (JMP®). Full details are shown in Table 1. In addition, the heat up and cool down total time in which the reaction temperature (121 °C) was reached in the autoclave and after lowering the temperature to 30 °C to be able to remove the reaction flask was 60 min.

The experiments were performed with 3 g of SB mixed with 30 mL of acidic solution. Temperature was taken to 121 °C using an autoclave (Yamato; model SK101C). After reaction time, each mixture was filtered (Whatman® No. 1 Paper) and washed with distilled water. The pH was adjusted to 4.9 ± 0.1 using a NaOH solution and a potentiometer (Hanna; model HI221). Finally, the substrate was dried in an oven at 35 °C for 24 h (Felisa; model FE-291). The dried biomass was stored at room temperature until further use. Additionally, one batch of un-washed pretreated biomass was dried and used for comparison purposes.

2.3. Severity factor

Ruiz et al. (2021) reported that the severity factor is an interesting parameter that can be applied during pretreatment processes for the biorefinery concept and size scaling up (Ruiz et al., 2021). The severity factor [log₁₀ (Ro)] provides information about the effects of specific pretreatment conditions including temperature and time. It has been observed that, when the severity factor increases, enzymatic hydrolysis of lignin is inhibited. It has been hypothesized that higher severity pretreatments indicate increased exposure and degradation of lignin. As a result, production of inhibitory compounds also increases. In the present work, the severity factor for acidic hydrothermal pretreated samples was calculated using Eq. (1), according to the methodology published by Ruiz et al. (2021). Eq. (1) can be used in pretreated solids rich in cellulose-lignin, according to SB composition.

$$\log R_0 = [R_0 \text{ Heating}] + [R_0 \text{ Isothermal process}] + [R_0 \text{ Cooling}] \quad (1)$$

$$\log R_0 = \left[\int_0^{t_{max}} \frac{T(t) - 100}{14.75} \right] + \left[\int_{ctrf}^{ctrf} \exp \left[\frac{(T(t) - 100)}{14.75} \right] dt \right] + \left[\int_0^{t_{max}} \frac{T(t) - 100}{14.75} \right] \quad (2)$$

Table 1

H₂SO₄ concentrations and reaction times used in the acid pretreatment at 121 °C.

Reaction time	Acid concentration (H ₂ SO ₄ (%v/v))		
	0.25	0.5	1.0
15 min	C 1	C 2	C 3
30 min	C 4	C 5	C 6
60 min	C 7	C 8	C 9

Where Ro is the modified severity factor; T(t) corresponds to the reaction temperature (in our case 121 °C) vs time profile. In addition, the *ctrf* and *ctrf* (min) terms correspond to the time needed for the whole heating-cooling period. In Eq. (1), “100” indicates the base temperature and 14.75 is the typical activation energy for glycosidic bond cleavage in carbohydrates, assuming a hydrothermal process occurs with a first order kinetics. Log₁₀ (Ro) corresponds to the final severity factor. In the present study, the severity factor was implemented for acidic pretreatment using a temperature of 121 °C and three times: 15, 30 and 60 min.

2.4. Enzymatic hydrolysis at micro-level: preparation of microreactors

SB enzymatic hydrolysis was performed at microscale level using the methodology previously reported by Molina et al. (2014). Before experiments, 10 mL of Cellic CTec 2® enzymatic solution were prepared according to Adney and Baker (2008). In addition, 100 mL of a buffer solution were adjusted to a pH value of 4.8. The solutions were stored at 4 °C until further use. For the micro-reaction, proper amounts of SB were added to 1.5 mL of phosphate buffer to obtain substrate concentrations of 10, 30, and 50 mg mL⁻¹ SB. Reaction tubes were placed in a thermomixer (Eppendorf brand; model ThermoMixer C) and heated to 50 °C. Later, the enzymatic solution was added to obtain enzyme concentrations of 10, 15, and 20 FPU/mL (See Table A1, Supplementary data). Reaction mixtures were stirred at 700 rpm (Molina et al., 2014) and allowed to react for 48 h. Aliquots were taken at 0, 6, 10, 24, and 48 h after hydrolysis started. Concentrations of reducing sugars were quantified using the Miller method (Miller, 1959). The enzymatic hydrolysis yield was calculated according to Delgado et al. (2009). For this purpose, we considered a complete reaction. The molecular weight (MW) of cellulose was taken as 162*n (where n is the number of glucose molecules per cellulose unit). Glucose displays a MW of 180. Thus, the stoichiometric factor ratio corresponds to 180/162 of released glucose per gram of cellulose. The maximum RS concentration can be calculated using Eq. (3):

$$MC_{RS} = \frac{180}{162} X_{ws} C_{ws} \quad (3)$$

where MC_{RS} is the maximum RS concentration (mg/mL); C_{WS} is the concentration of dry SB in the enzymatic hydrolysis media (mg/mL); and X_{WS} is the fraction of cellulose + hemicellulose in the dry substrate. Enzymatic hydrolysis yield was calculated according to Eq. (4):

$$\text{Enzymatic hydrolysis yield} = \frac{RS_C}{MC_{RS}} \times 100 \quad (4)$$

2.5. Enzymatic hydrolysis at micro-level: acidic concentration vs reaction time on hydrolysis yield

The micro-enzymatic hydrolysis was performed to determine the effect of acid concentration vs reaction time on RS production. The objective of this experiment was to evaluate the pretreatment conditions that increase RS yield during EH. In addition, valuable data for further scaling up processes were obtained. A 3² factorial design (JMP®) was used to study the effects of acidic concentration and reaction time on the hydrolysis yield. Acid concentration (X1), ranging from 0.25% to 1% (v/v), and reaction time (X2), between 15 and 60 min, were the independent variables scrutinized in this work. The experiments were carried out in triplicate as independent experiments in order to take into account the non-adjustable data and allow the calculations of the analysis of variance (ANOVA). The ranges and levels of independent input variables are shown in Table 1.

2.6. Enzymatic hydrolysis at micro-level: enzyme concentration vs biomass concentration on hydrolysis yield

The micro-enzymatic hydrolysis was also performed to determine

the effect of solid loading vs enzyme concentration on RS production. A 3² factorial design (JMP ®) was used to study the effects of enzyme concentration and solid loading on the hydrolysis yield. Enzyme concentration (X1), ranging from 10 to 20 FPU/mL, and biomass concentration (X2), between 10 and 50 mg/mL, were the independent variables scrutinized in this work. The experiments were carried out in triplicate as independent experiments in order to take into account the non-adjustable data and allow the calculations of the analysis of variance (ANOVA). The ranges and levels of independent input variables are shown in Tables 3 and 4 for alkali and acid pretreatment, respectively.

2.7. Bioethanol production: culture conditions

In the present study, *Kluyveromyces marxianus* was used to produce bioethanol 2G. Lyophilized *K. marxianus* was gently donated by the company CHR HANSEN®, and before experiments, yeast cells were reactivated. After reactivation, cells were inoculated on YPD agar containing 20 g L⁻¹ peptone, 10 g L⁻¹ yeast extract, 20 g L⁻¹ D-Glucose, and 15 g L⁻¹ agar. Afterwards, microorganisms were incubated at 30 °C for 48 h (Sandoval-Nuñez et al., 2017). Preinoculum was prepared by transferring a yeast colony to YPD medium to achieve a ratio of 1:2.5. Incubation was carried out at 30 °C and 250 rpm for 24 h as described in Sandoval-Nuñez et al. (2017). The growth of *K. marxianus* was measured using a Neubauer chamber and associated to optical density (600 nm).

2.8. Scale up of pretreatment, enzymatic hydrolysis, and fermentation

2.8.1. Pretreatment

For these experiments, pretreatments that resulted in the best yield were selected. These treatments corresponded to: (AP1) 121 °C, 15 min, and 0.5% acid (v/v); and (AP2) 121 °C, 30 min, and 1% of acid (v/v). Herein, 80 g of dry SB (10% w/w) were placed in a 2 L Erlenmeyer flask, followed by 800 mL of the corresponding diluted acid solution, and autoclaved using a Yamato autoclave (model SK101C). After pretreatment, SB pH was adjusted to 5 ± 0.2 using a NaOH solution. Later, the mixture was filtered, and the humidity was determined with a thermobalance (RADWAG; PMR model 50/1). The enzymatic hydrolysis was performed immediately.

2.8.2. Enzymatic hydrolysis

The enzymatic hydrolysis (EH) of pretreated biomass was carried out in a 3 L reactor (Applikon; 3 L single wall autoclavable model) with a loading of 10% of solids and operational volume of 800 mL. For this purpose, 80 g of pretreated SB and 800 mL of buffer were placed in the bioreactor, and pH was adjusted to 5.0 ± 0.2 using a portable potentiometer (Hanna; model HI98190). The reactor was equipped with a thermal insulator to mitigate heat dissipation. Temperature was maintained at 50 °C and mixing velocity at 250 rpm. Once proper temperature was reached, Cellic CTec 2® enzyme was added to obtain a concentration of 3%, which corresponds to 11.07 FPU/g cellulose. Samples were taken at the beginning of the reaction and every 2 h for 24 h. Resulting samples were analyzed using high performance liquid chromatography (HPLC) and gas chromatography (GC) according to Amaya-Delgado et al. (2013).

2.8.3. Fermentation experiments

Fermentation was conducted immediately after EH finished. Experimental conditions included a temperature of 30 °C and 75 rpm. Before fermentation started, the reaction broth was enriched with the following components (g L⁻¹): 0.1 yeast extract, 0.5 dibasic sodium phosphate, and 0.1 magnesium sulfate. Afterwards, the reactor was inoculated with 20 million *K. marxianus* yeast cells, which were quantified using a Neubauer chamber. The pH was adjusted to 5.0 ± 0.2. Finally, samples were taken every 2 h during 24 h. The samples were analyzed using high performance liquid chromatography (HPLC).

2.9. Distillation

The reaction broth was distilled. The simple-distillation device was equipped with a reboiler at the bottom of the column and a condenser in the dome. In order to cool down the distillate, the recirculator (Julabo; model F 25) was placed on iced water at a temperature of 10 ± 5 °C. Distillate was collected in a 100 mL beaker. Samples were stored in 50 mL Falcon™ conical tubes for further GC analysis.

2.10. Analytical methods

2.10.1. Gas chromatography

Quantification of ethanol and volatile compounds was carried out using an Agilent Gas chromatograph (model 7890B) (GC) with a flame ionization detector, coupled to a head-space autosampler (Model 7697A). In order to separate the components, an HP Innnowax column (60 m × 0.32 mm × 0.25 µm) was used at a pressure of 23,787 psi and a flow of 1.3 mL/min to obtain a speed of 24,502 cm/s. Furnace heating started at 45 °C for 8 min and then was heated for 10 min at a rate of 2 °C min⁻¹ to reach a temperature of 80 °C. Subsequently, the T increased at a rate of 5 °C min⁻¹. Later, reaction mixture was maintained at a T of 160 °C for 10 min. Afterwards, a rate of 25 °C min⁻¹/4 min allowed the mixture to reach a T of 220 °C. The detector temperature was 250 °C and gas flow rates were 40, 400, and 30 mL min⁻¹ for helium, air, and nitrogen, respectively. The headspace was programmed under the following conditions: vial temperature of 90 °C for 5 min; loop temperature of 110 °C; transfer line temperature of 115 °C; equilibration time of 5 min; injection time of 0.5 min; and cycle time of 60 min. The calibration curve with 15 intermediate points was built from 1 to 1000 ppm for acetaldehyde, isobutyraldehyde, ethyl acetate, methanol, ethanol, ethyl butyrate, 1-propanol, isoamyl acetate, isobutanol, isopentyl acetate, isoamyl alcohol, ethyl hexanoate, ethyl lactate, ethyl octanoate, ethyl decanoate, 2-3 butanedione, and 2-phenyl ethanol.

2.10.2. High performance liquid chromatography (HPLC)

The quantification of sugars was carried out using a high-performance liquid chromatograph (HPLC) (Agilent brand; Model 1220 Infinity) equipped with a refractive index detector (RID), a UV detector, and a Biorad Aminex HPX-87H column (300 mm × 7.8 mm, 9 µm). The column was maintained at 50 °C and 5 mM H₂SO₄ was used as the mobile phase at a flow rate of 0.5 mL/min for 30 min. For sample preparation purposes, 1 mL of hydrolyzed sample was taken with a syringe and filtered using a 0.45 µm Agilent® Nylon filter. Later, the filtered samples were placed in HPLC vials and closed with a white silicone lid.

2.10.3. X-ray analysis

Crystal sizes before and after chemical pretreatment and enzymatic hydrolysis were determined using an X-ray diffractometer (Panalytical Brand; Empyrean model, USA) at 45 kV and 40 mA, taking the Cu K α line as reference with a wavelength of 1.54 Å. For analysis, 1 g SB was mounted on a special aluminum sample holder and placed in the diffractometer. Samples were scanned between 10° and 45° (2 θ) with intervals of 0.020°. The crystallinity index was calculated using Eq. (5), according to Segal et al. (1959):

$$CrI = \frac{(I_{002} - I_{AM})}{I_{002}} \times 100 \quad (5)$$

Where I_{002} and I_{AM} correspond to the intensity of the crystalline and amorphous phase at 22.7° and 18° in 2 θ , respectively.

Crystallite size was calculated considering a direction perpendicular to its Miller plane using the Scherrer equation (Eq. 6):

$$t_{002} = \frac{K\lambda}{\beta_{002}\cos\theta} \quad (6)$$

Where t_{002} indicates crystallite size in Miller plane 002; λ is an x-ray wavelength ($\lambda = 0.154$ nm for $\text{CuK}\alpha$); θ is the Bragg angle of the reflection (radians); β_{002} is the pure integral of the reflection width at one half maximum height in the 002 plane (radians); and K is the Scherrer constant, which was considered as 1.

X-ray fluorescence was used to determine the content of silica. For this purpose, an XRF equipment (Panalytical Brand; Epsilon 3-XL model) was used with an Ar atmosphere and an Rh tube at 20 kV and 0.1 mA. Before measurements, 1 g of each sample was placed in 32 mm sample holders.

2.10.4. Scanning Electronic Microscopy (SEM) analysis

Morphological analysis of samples was carried out through Scanning Electron Microscopy (SEM) (JSM-6510LV, JEOL). The SB samples were placed on Carbone type. The SEM was operated at 20 kV and images were acquired at $800\times$.

2.10.5. Total Attenuated Reflection (ATR) (Infra-Red)

The functional groups present in biomass (a) before pretreatment; (b) after pretreatment; and (c) after enzymatic hydrolysis were identified using ATR analysis. The infrared spectra were collected on an ATR spectrometer (Agilent, model: Cary 630; USA). The ATR spectra were collected in absorption band mode in the range of $800\text{--}4000$ cm^{-1} with a resolution of 4 cm^{-1} and 32 scans.

2.11. Mass and energy balance and reactor volume

The mass and energy balance for the fundamentals stages of bio-ethanol production were performed. Herein, for mass balance, we selected a basis of $18,750$ kg h^{-1} , taking into account the pretreatment, enzymatic hydrolysis, and fermentation reactors. The plant design considered the complete process for ethanol production. In order to estimate the reactors size, we considered the experimental data about cellulose, hemicellulose, and lignin content before and after diluted sulfuric acid pretreatment, EH, and fermentation. The volume of the pretreatment reactor was calculated considering the inlet volumetric flow minus the outlet volumetric flow as well as biomass density. This result was multiplied by the residence time. Finally, the reactor considered an overdesign of 20% according to Eq. (7):

$$\text{Volume} = 1.2 * \left(\frac{\text{Total mass flow}}{\text{Water density}} \right) + \left(\frac{\text{Total mass flow}}{\text{Biomass density}} \right) - \left(\frac{\text{Outlet mass flow}}{\text{Biomass density}} \right) * rt \quad (7)$$

Where rt represents the reactor residence time. The biomass density was considered as 190 kg m^{-3} according to Wild and Visser (2018). Calculations for the volume of the enzymatic hydrolysis reactor considered the composition of the pretreated biomass at the reactor feeding point. At the reactor discharge point, the experimental results for glucose and xylose production were also considered. The experimental data were fitted to a regression model in order to obtain the conversion performance of cellulose and hemicellulose. The volume was calculated by means of Eq. (7). Finally, the volume of the fermenter was calculated considering the concentrations of glucose and xylose previously obtained. The experimental data were also fitted to a regression model to obtain the glucose and xylose conversion yields. Within calculations, the change in density was adjusted using a regression model.

The energy balance was performed according to Seader and Henley (2011), considering the calculated volume of the reactor as well as the operative conditions necessary to maintain a certain reactor temperature during the process. In the case of the pretreatment reactor, we proposed that 10% of the total volume corresponded to steam.

3. Results and discussions

3.1. Composition of sotal fibers

In order to quantify structural carbohydrates present in SB, we used the method reported in Sluiter et al. (2011). Our data indicated that cellulose, hemicellulose, and lignin content in untreated SB was 311.4 , 31.1 , and 350.42 g kg^{-1} of cellulose, hemicellulose, and lignin, respectively. In the case of SB exposed to alkali (NaOH), resulting composition was 474.7 , 79.6 , and 168.2 g kg^{-1} , correspondingly. With respect to SB pretreated with diluted sulfuric acid (H_2SO_4), numbers were 542.2 , 30.3 , and 250.2 g kg^{-1} , in the same order.

The results demonstrated an increase in 52.5% and 74% in cellulose content when samples were exposed to alkali and acid pretreatment, respectively, as compared to untreated samples. A 155.9% increase and 2.5% decrease in hemicellulose content was observed after alkali and acid pretreatment, correspondingly, as compared to controls. In addition, data indicated that alkali pretreatment resulted in a higher delignification ratio (52%), as compared to the one obtained with acid pretreatment (28.59%). Our delignification results using alkali pretreatment were higher than those obtained for rice straw (28.4%; @6% of NaOH), and lower than those resulting using an alkaline-oxidative pretreatment on agave bagasse (82.62) where high quantities of reagent and high temperatures were applied. In the case of the acid pretreatment, previous reports have indicated a 19.6% delignification rate when agave bagasse was exposed to oxidative pretreatment using a relatively long reaction time of 48 h. In this case, delignification was lower than the one obtained in the present work (Perez-Pimienta et al., 2013). Other reports have indicated that a sequential acid-alkali pretreatment on leaves of the desert plant *Agave salmiana* resulted in a delignification yield of 84%, which is higher than those obtained in our work using SB (Láinez et al., 2019).

3.1.1. Effect of acidic concentration vs reaction time on hydrolysis yield

The objective of this experiment was to evaluate the conditions that maximize RS yield during EH. In addition, valuable data for further scaling up processes were obtained. Table 2 shows the effect of operating conditions on RS production. The p -value of the adjusted model ($p < 0.0001$) indicated that the model was significant, and the lack of fit was insignificant ($p = 0.0876$). Therefore, the statistical analysis demonstrated that the selected model properly described the response ($R^2 = 0.88$ and adjusted $R^2 = 0.83$). Results indicated that the optimal value was obtained when a reaction time of 15 min and H_2SO_4 concentration of 0.5 (v/v) were used. With respect to EH of pretreated SB samples, the Analysis of variance (ANOVA) showed that time, acid concentration, and the interaction among time and acid concentration were significant factors affecting production of reducing sugars. The variable "acid concentration" showed a higher significance in the pretreatment process (see Supplementary data) with respect to others. The severity factor obtained for this treatment was the lowest (2.78). As previously reported, the severity factor depends on the type of pretreatment (Chundawat et al., 2008). However, it has been observed that, when the severity factor increases, the resulting lignin presents a higher inhibition of enzymatic hydrolysis (Ruiz et al., 2021). Table 2 depicts the EH results for pretreated sotal bagasse samples. The higher RS

Table 2
RS production during enzymatic hydrolysis (10 FPU/mL) at micro level scale of acid pretreated samples.

Reaction time (min)	Acid concentration (H_2SO_4 (%v/v))			Severity factor
	0.25	0.5	1.0	
15	$3,39 \pm 0,25$	$4,9 \pm 0,75$	$3,96 \pm 0,35$	2.78
30	$3,68 \pm 0,25$	$3,43 \pm 0,55$	$4,1 \pm 1,01$	2.86
60	$3,34 \pm 0,75$	$3,35 \pm 0,35$	$4,4 \pm 1,00$	2.99

concentration (4.9 ± 0.75 mg/mL) was obtained with a severity factor of 2.78. In addition, a severity factor of 2.99 resulted in the lowest RS concentration (3.35 ± 0.35 mg/mL), which was probably associated to the presence of inhibitory compounds. We labeled experimental conditions of 15 min and 0.5% H₂SO₄ (v/v) as AP1. This last experiment was selected for further scale up. In addition, a trend analysis was performed ($\text{Prob} > |t|$). Thus, we decided to evaluate an experiment following the observed trend using a time of 30 min and a concentration of 1% H₂SO₄ (v/v). These conditions were labeled AP2 (see Supplementary data). Finally, as it was previously reported, high temperatures increase the breakage of cellulose units. Pino et al. (2019) reported that temperatures between 160 and 220 significantly increased RS concentrations. On the other hand, time does not significantly affect the yield of reducing sugars. Pino et al. (2019) reported that optimized RS yield occurred at 194 °C and 30 min of reaction.

3.1.2. Micro-scale level: effect of enzyme concentration vs biomass concentration on EH yield

Our results for EH of alkali and acid pre-treated SB samples at the micro-scale level are shown in Tables 3 and 4. Table 3 presents a comparison of the results obtained for SB samples pretreated with an alkaline solution for washed and unwashed biomass. Results indicated that after EH, RS concentration in the samples increased as enzyme concentrations also increased. This result indicated that the production of RS was favored when the amount of enzyme in the reactor increased ($10 < 15 < 20$ FPU). This trend was observed for both, washed and unwashed biomass. However, when the amount of biomass increased from 10 to 50 mg and the enzyme concentration did not change, a decrease in RS concentration was observed for both, washed and unwashed biomass. These data indicated that the increase in biomass in the reactor decreased the reaction yield. The RS production was favored when a relatively low biomass content was present ($10 > 30 > 50$ mg mL⁻¹). In addition, after alkaline treatment, reaction yield decreased from 20.1% to 3% when the amount of unwashed biomass increased from 10 to 50 mg mL⁻¹ at an enzyme concentration of 10 FPU. The same trend was observed for washed biomass using an enzyme concentration of 10 FPU. In this case, yield decreased from 37.8% to 4.5% at biomass concentrations of 10 and 50 mg mL⁻¹, respectively. Comparing the results for washed and unwashed biomass, it was concluded that a higher EH yield was obtained when alkaline pretreatment and washed biomass were used. Our results were similar to those reported for wheat straw (WS) (Molina et al., 2014).

The *p*-value of the adjusted model ($p < 0.0001$) implied that model fitting was significant, and the lack of fit was insignificant ($p = 0.0604$). Therefore, the statistical analysis demonstrated that the model properly described the response ($R^2 = 0.955$ and adjusted $R^2 = 0.951$). The linear and quadratic terms for enzyme concentration were statistically significant ($p < 0.05$). The regression coefficients showed that enzyme concentration presented a positive effect on the overall sugar yield. In addition, increasing amounts of biomass in the microreactor displayed a

negative effect on sugar yield. The Analysis of variance (ANOVA) for production of reducing sugars showed that enzyme and biomass concentration, as well as the interaction between enzyme and biomass concentration, significantly affected the final concentration of reducing sugars obtained during EH of pretreated SB samples. The enzyme concentration in the bioreactor significantly affected the process (see Supplementary data).

Table 4 presents the results for the EH of SB pretreated with diluted acid using washed and unwashed biomass. In the case of unwashed biomass, our data indicated an increase in RS concentration when the enzyme concentration increased from 10 to 20 FPU. In addition, an increase in RS production occurred when biomass concentration increased; however, the yield decreased significantly. Reaction yields of 33.5%, 19.2%, and 13.4% were obtained for biomass concentrations of 10, 30, and 50 mg mL⁻¹, respectively. These results indicated that reaction yield decreased at higher biomass concentrations ($10 > 30 > 50$ mg mL⁻¹). In the case of washed biomass, data indicated that RS concentrations increased when enzyme content increased from 10 to 20 FPU. It was also observed that reaction yield decreased from 32.8% to 10.4% when biomass contents were of 10 mg and 50 mg, respectively. Thus, a similar or superior reaction performance was obtained when unwashed biomass was used.

The *p*-value of the adjusted model ($p < 0.0001$) implied that model fitting was significant, and the lack of fit was insignificant ($p = 0.025$). Therefore, our statistical analysis demonstrated that our model properly described the response ($R^2 = 0.990$ and adjusted $R^2 = 0.986$). The linear and quadratic terms of enzyme concentration and biomass were statistically significant model terms ($p < 0.05$). The regression coefficients showed that enzyme concentration positively affected overall sugar yield, while the increase in biomass content in the microreactor displayed a negative effect on the overall sugar yield as previously reported by Aguirre-Fierro et al. (2020). The Analysis of variance (ANOVA) for production of reducing sugars showed that enzyme and biomass concentration, and the interaction between enzyme and biomass concentration significantly affected the concentration of reducing sugars obtained in EH of pretreated SB samples. The biomass in the microreactor significantly affected RS production (see Supplementary data).

Comparing the EH results for SB with alkaline and acid treatment, it was observed that the highest RS concentrations and reaction yields were obtained for AP unwashed biomass. This result could be associated with the quantification of by-products obtained during AP. For this reason, this material was selected for the scale up experiment.

3.2. Experiments at 1L scale

3.2.1. Pretreatment and enzymatic hydrolysis

After data analysis, the selected operative conditions for SB pretreatment were: (a) 0.5% v/v, 15 min, and 120 °C (AP1); (b) 1.0% v/v, 30 min, 120 °C (AP2). After pretreatment, SB was dried until a 10% moisture content was achieved. Figs. 1a and 2a present the results for

Table 3
RS produced after EH of alkali pretreated biomass.

Enzyme concentration (FPU/mL)	RS produced (mg/mL) (Unwashed)			Yield (Unwashed)		
	Biomass in micro reactor (mg)					
	10	30	50	10	30	50
10	2.010 ± 0.053	1.530 ± 0.056	1.490 ± 0.056	20.1%	5.10%	3.00%
15	2.850 ± 0.050	2.610 ± 0.036	2.437 ± 0.072	28.5%	8.70%	4.90%
20	4.450 ± 0.133	4.410 ± 0.161	3.910 ± 0.107	44.5%	14.7%	7.80%
Enzyme concentration (FPU/mL)	RS produced (mg/mL) (Washed)			Yield (Washed)		
	Biomass in micro reactor (mg)					
	10	30	50	10	30	50
10	3.780 ± 0.002	2.320 ± 0.004	2.230 ± 0.001	37.8%	7.70%	4.50%
15	4.053 ± 0.037	2.825 ± 0.084	2.913 ± 0.051	40.5%	9.40%	5.80%
20	5.180 ± 0.009	4.580 ± 0.001	4.710 ± 0.002	51.8%	15.3%	9.40%

Table 4

RS produced after EH of acid pretreated biomass (AP1).

Enzyme concentration (FPU/mL)	RS produced (mg/mL)			Yield		
	(Unwashed)			(Unwashed)		
	Biomass (mg)					
	10	30	50	10	30	50
10	3.297 ± 0.039	6.057 ± 0.323	6.133 ± 0.292	33.5%	19.2%	13.4%
15	3.437 ± 0.072	5.443 ± 0.175	6.695 ± 0.008	34.8%	18.1%	13.4%
20	5.783 ± 0.034	7.050 ± 0.058	7.180 ± 0.040	57.8%	23.5%	14.4%
Enzyme concentration (FPU/mL)	RS produced (mg/mL)			Yield		
	(Washed)			(Washed)		
	Biomass (mg)					
	10	30	50	10	30	50
10	3.280 ± 0.004	3.990 ± 0.002	5.190 ± 0.003	32.8%	13.3%	10.4%
15	3.483 ± 0.059	4.753 ± 0.004	5.653 ± 0.279	34.8%	15.8%	11.3%
20	4.833 ± 0.018	6.043 ± 0.005	6.580 ± 0.002	48.3%	20.1%	13.2%

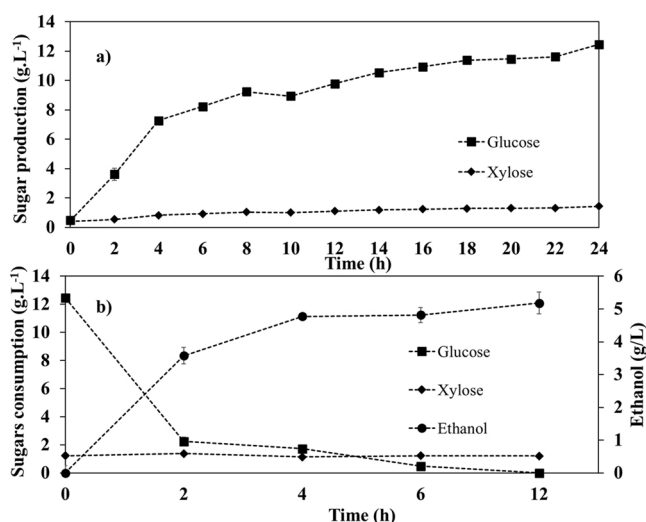


Fig. 1. a) Glucose and xylose production during scale up experiments; b) Sugar consumption and ethanol production. Biomass was pretreated with 0.5% H₂SO₄ for 15 min.

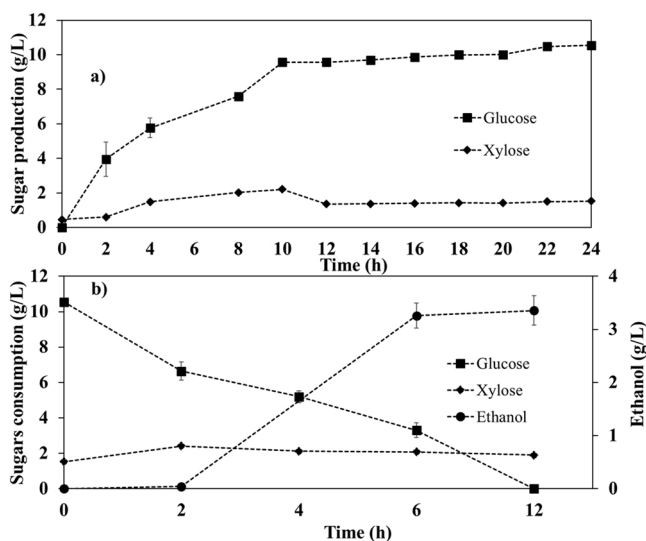


Fig. 2. a) Glucose and xylose production during scale up experiments; b) Sugar consumption and ethanol production. Biomass was pretreated with 1% H₂SO₄ for 30 min.

glucose and xylose production after EH of acid pretreated SB. According to the supplier's instructions, EH was carried out for 24 h at a solid load of 10% and an enzyme concentration of 11 FPU (3% w/w Cellic Ctec 2®). Selected pretreatment conditions were as follows: 0.5% H₂SO₄ and 15 min (Fig. 1a); 1% H₂SO₄ and 30 min (Fig. 2a). Our results indicated that the highest sugar production was obtained with biomass pretreated with 0.5% acid, where glucose and xylose concentrations were 12.5 ± 0.25 and 1.4 ± 0.02 g L⁻¹, respectively (Fig. 1a). In the case of biomass pretreated with 1% H₂SO₄, results were 10.54 ± 0.07 and 1.5 ± 0.02 g L⁻¹ (Fig. 2a), correspondingly. This concentration represented a total RS yield of 22.4% (Fig. 1a) and 19.46% (Fig. 2a) after EH reaction. Calculations were performed considering 80 g of SB (10% solids load) with a 69.58% fraction of cellulose + hemicellulose.

Performance was calculated as reported by Molina et al. (2014). The severity factor displayed values of 2.78 and 2.86 for AP1 and AP2, respectively. As it is possible to notice, the concentration of reducing sugars was lower when increasing the severity factor in AP2, which is consistent with that reported in Ruiz et al. (2021). According to our results, reaction yield was relatively high as compared to that obtained using micro-reaction with concentrations of 30 and 50 mg SB and enzyme levels of 10 and 15 FPU. The yield was lower than that obtained at enzyme concentrations of 10 mg and 15 FPU. The low performance observed during scale up may be associated with deficiencies in heat and mass transfer.

Table 5 presents the yields of enzymatic hydrolysis at micro-scale and bench-scale level using different types of biomass, including the SB used in the present research. Data show that microscale acid and alkaline pretreatments presented a maximum yield of 57.8% and 51.8%, respectively. The enzymatic hydrolysis performed during scaling up using the acidic pretreatments AP1 and AP2 were 22.4% and 19.46%, respectively.

Compared with other reports of enzymatic hydrolysis using different pretreated material, Agave bagasse hydrolysates pretreated with acid displayed yield of 34% when a yeast mixture was used (Celluclast 1.5L® and Novozyme 188®.) (Saucedo-Luna et al., 2011). This value was smaller as that obtained in our research in microreaction. Other substrates including sugarcane bagasse and wheat straw (Sandoval-Nuñez et al., 2017) presented yields of 46% and 42%, respectively, which were also smaller than the yields produced in the micro-reaction used in the present work.

Other researchers have used industrialized desertic plant residues including agave bagasse (See Table 5), and applied different pretreatment methodologies including alkali extrusion, organosolv, acid hydrolysis, autohydrolysis, and ionic liquids, as well as several pretreatment combinations. Montiel et al. (2016) reported a saccharification yield of 73% when agave bagasse was subjected to a combined alkali extrusion-saccharification process using 80% of Cellic Ctec 2® and 20% of Vizcozyme (Montiel et al., 2016). In addition, Avila Lara et al. (2015), obtained a saccharification yield of 74.4% after alkaline pretreatment of Agave bagasse and subsequent EH with 35 FPU/g Cellic

Table 5
Results comparison with other works using different AIW and pretreatment-hydrolysis conditions.

Substrate	Pretreatment conditions	Enzyme employed	Hydrolysis yield	Reference
Agave <i>lechuguilla</i> heart (cogollos)	Sequential 72% (v/v) H ₂ SO ₄ ; 30 °C; 60 min then 121 °C; 4% H ₂ SO ₄ per 60 min. Then autohydrolysis at 190 °C per 30 min	Accellerase 1500®	60.85%	(Ortíz-Méndez et al., 2017)
Leaves of Agave <i>salmiana</i>	Sequential 1% (v/v) H ₂ SO ₄ , for 90 min then 3.4% (v/v) of NaOH for 70 min, both at 121 °C	Celluclast 1.5 L (Novozyme). (5 FPU/g cellulose)	85%	(Láinez et al., 2019)
Agave bagasse (<i>tequilana weber</i>)	147 °C; 2.3% H ₂ SO ₄ ; 15 min	Celluclast 1.5 L® and Novozyme 188®.	37.4%	(Saucedo-Luna et al., 2011)
Agave bagasse	NaOH/Extrusion	80% of Cellic CTec 2® and 20% of Vizcozyme	73%	(Montiel et al., 2016)
Agave bagasse	130 °C; 1.58% H ₂ SO ₄ ; 52.5 min	Cellic® CTec2 and HTec2	57.6%	(Ávila-Lara et al., 2015)
Agave <i>salmiana</i> bagasse	120 °C; ionic liquid [C2C1Im][OAc]; 3 h.	Not specified	23.3%	(Pérez-Pimienta et al., 2018)
Agave <i>fourcroydes</i>	120 °C; ionic liquid [C2C1Im][OAc]; 3 h.	Not specified	49.2%	(Pérez-Pimienta et al., 2018)
Agave bagasse	Not pretreated	(Celluclast 1.5 L/Viscozyme L and Cellic® Ctec2/Cellic® Htec2	31.25%	(López-Gutiérrez et al., 2020)
Sugarcane bagasse	121 °C; 2% H ₂ SO ₄ ; 15 min	HTec2 and CTec2 from Novozyme®.	46%	(Sandoval-Núñez et al., 2017)
Wheat straw	121 °C; 2.3% H ₂ SO ₄ ; 15 min	HTec2 and CTec2 from Novozyme®.	42%	(Sandoval-Núñez et al., 2017)
Sotol bagasse (Microreaction)	121 °C; 0.5% H ₂ SO ₄ ; 15 min	Cellic CeTec2®	57.8%	This work
Sotol bagasse (Microreaction)	30 °C; 6% NaOH; 6 h	Cellic CeTec2®	51.8%	This work
Sotol bagasse (800 mL)	121 °C; 0.5% H ₂ SO ₄ ; 15 min	Cellic CeTec2®	22.4%	This work

CTec 2® (Ávila-Lara et al., 2015). Furthermore, Perez-Pimienta et al. (2013) achieved a saccharification yield of 53.80% after 72 h of reaction with the application of acid hydrolysis and EH using 8 FPU/g Cellic CTec 2® and 15 CBU/g Cellic HTec 2® (Perez-Pimienta et al., 2013). Different agave biomasses have been pretreated with ionic liquids. For example, Perez-Pimienta et al. (2018) treated *Agave salmiana* bagasse and *Agave fourcroydes* with the ionic liquid [C2C1Im][OAc] per 3 h at 120 °C, reporting hydrolysis yields of 23.3% and 49.2%, respectively. Also, in one hand, sequential treatments have been tested for the treatment of heart of *Agave lechuguilla* and leaves of *Agave salmiana*. Ortíz-Méndez et al. (2017) evaluated the sequential pretreatment of heart of *Agave lechuguilla* heart, which was exposed to 72% (v/v) H₂SO₄ at 30 °C for 60 min, followed by a 60 min treatment with 4% (v/v) H₂SO₄ and finally an autohydrolysis at 190 °C for 30 min. According to their reports, these researchers obtained a saccharification yield of 55% (Ortíz-Méndez et al., 2017). Another sequential pretreatment was used by Láinez et al. (2019), who exposed leaves of *Agave salmiana* to 1% (v/v) H₂SO₄ for 90 min at 121 °C, followed by 3.4% (v/v) NaOH for 70 min, also at 121 °C. A final saccharification with Celluclast 1.5 L (Novozyme ®) produced a hydrolysis yield of 85%.

3.2.2. Fermentation experiments

Figs. 1b and 2b present the fermentation results. In this case, experiments were monitored for 12 h. After reaction time, ethanol production was $5.18 \pm 0.3 \text{ g L}^{-1}$ (F1) and $3.3 \pm 0.2 \text{ g L}^{-1}$ (F2) for the fermentations performed with hydrolyzed biomass obtained from AP1 (Fig. 1b) and AP2 (Fig. 2b), respectively. These results were similar to those reported by Sandoval-Núñez et al. (2017) using *K. marxianus*. Fermentation yields were 81.09% and 61.27% when hydrolyzed biomass obtained from AP1 (Fig. 1b) and AP2 (Fig. 2b) were used, respectively. The fermentation yield was calculated according to Láinez et al. (2019). In addition, the fermentation rate 0.41 g/g for AP1 was similar to that reported in Sandoval-Núñez et al. (2017). Data indicated that the yeast *K. marxianus* was not able to catabolize xylose. This probably occurred because pH negatively affected the microorganism metabolism. According to the results shown in Fig. 1b, *K. marxianus* did not consume xylose during the experiments. This means that xylose will be part of the distillation residues called vinasse. Thus, in order to obtain further added-value products such as biopolymers, additional

bioprocesses may be implemented (Ferraresi de Araujo and Niño-Castillo, 2021). After fermentation experiments, the reaction broth was filtered in order to separate the cake and the liquid phase. This liquid was later distilled, and the chemical composition was determined using GC. The chromatographic analysis showed the presence of ethanol as the major product, and acetaldehyde in relatively low concentrations (fermentation F1 (Fig. 1b)); however, no fermentation inhibition was observed. In the case of fermentation F2 (Fig. 2b), results indicated the presence of ethanol as the major product, and acetaldehyde, methanol, iso-butanol, and isoamyl alcohol, in lower ratios. Herein, fermentation inhibition occurred. The production of these compounds during the fermentation process may be associated with the presence of different inhibitors including furfural or hydroxymethyl furfural (HMF) that can be related with a higher value (2.86) of severity factor, that was previously reported in Ruiz et al. (2021). These compounds produce oxidative stress in the microorganisms and deviate the metabolism to produce acetaldehyde, iso-butanol, and isoamyl alcohol. The effect of compounds such as furfural or HMF on the metabolism of *K. marxianus* has been previously reported in Flores-Cosío et al. (2018). Chromatograms are included in the Supplementary data.

The ethanol concentration obtained in the present research was similar to that obtained by Sandoval-Núñez et al. (2017) when *K. marxianus* was used along with WS hydrolysates. Sandoval-Núñez et al. (2017) obtained 5.1 g L^{-1} ethanol when fermentation was performed in the absence of inhibitory byproducts. In addition, these investigators reported a lower ethanol yield (3.1 g L^{-1}) when fermentation was done with WS hydrolysates in the presence of different inhibitory compounds including some phenolic compounds, furan derivatives (furfural and HMF), and aliphatic carboxylic acids (acetic acid) (Sandoval-Núñez et al., 2017). Other authors have reported that fermentation of acid pretreated *Agave tequilana* bagasse resulted in 24 g L^{-1} reducing sugars and 6.37 g L^{-1} ethanol. In this case, these researchers used the yeast *Pichia caribbica* (Saucedo-Luna et al., 2011).

The severity factor is related to the presence of inhibitory byproducts generated through fermentation. The biomass obtained from the experiment labeled AP2 (with a SF 2.86) was fermented in the presence of *K. marxianus*. The results showed an inhibitory response during EH and its subsequent fermentation. Also, different by-products including iso-amyl alcohol and iso-butanol, among others, were identified. It has

been reported that the metabolism of *K. marxianus* produces these compounds in the presence of furfural or hydroxymethyl furfural. These results allow to select the adequate biomass pretreatment associated with the severity factor and its posterior scaling up.

3.3. Mass and energy balance

The fundamental stages for a biorefinery design are shown in Fig. 3, along with operating conditions. Main stages include pretreatment, enzymatic hydrolysis, and fermentation. In our investigation, only one scenario was evaluated. Pretreatment was performed with a residence time of 15 min. Both, reactor temperature and sulfuric acid concentration are shown in Fig. 3. The reactor volume was calculated using 18,750 kg h⁻¹ as feedstock basis. The composition of the biomass was 5838.75, 583.13, and 6641.25 kg h⁻¹ of cellulose, hemicellulose, and lignin, respectively. In addition, the pretreatment reactor effluent presented a mass flow of 3346.83, 186.35, 1538.73, 2491.92, and 396.78 kg h⁻¹ for cellulose, hemicellulose, lignin, glucose, and xylose, respectively. The volume of the pretreatment reactor was 27.22 m³.

During calculations of the EH reactor volume, the composition of the pretreatment reactor effluent was considered. The enzyme concentration was achieved using a 3% of Cellic CTec 2®. Concentrations of cellulose, hemicellulose, lignin, glucose, and xylose in the EH effluent were 2660.73, 183.55, 1538.73, 3178.02, and 399.58 kg h⁻¹, respectively. The calculated EH reactor volume was 104.42 m³.

In order to calculate the fermenter volume, we only considered the amounts of glucose and xylose produced in the EH. In addition, reactor operating conditions were 30 °C and residence time of 8 h. This time was considered because of the low ethanol production after this period. The composition in the fermenter effluent was 2864.49, 365.5, and 347.63 kg h⁻¹ of ethanol, glucose, and xylose, respectively. Resulting fermenter volume was 693.68 m³.

The energy and mass yields were calculated according to Morales et al. (2021) considering an ethanol density of 0.79 kg L⁻¹ and an energy content of 26.8 MJ kg⁻¹ ethanol. According to mass balance data, the potential energy that may be produced using the resulting bioethanol was 76,768.33 MJ h⁻¹. In the present work, the ratio of bioethanol and energy produced per kg dry SB were 0.19 L (0.15 kg), and 4.09 MJ, respectively. The rate of bioethanol production obtained in the present research was lower than that reported using hardwood chips (0.25 L kg⁻¹) (Cardona Alzate and Sánchez Toro, 2006). Furthermore, the amount of bioethanol produced in our experiments (0.15 kg kg⁻¹) was similar to that reported for softwood forest residues (0.19 kg kg⁻¹ DB) (Karlsson et al., 2014). In addition, the energy content reported herein (4.09 MJ kg⁻¹) was lower than those obtained for switchgrass (5.43 MJ kg⁻¹), hardwood chips (5.29 MJ kg⁻¹), and *E. globulus* (8.93 MJ kg⁻¹) (Cardona Alzate and Sánchez Toro, 2006; Montiel et al., 2016; Saucedo-Luna et al., 2011).

According to our results, 49,755.62, 8.74, and 11.61 MJ h⁻¹ are needed to properly run the pretreatment tank, EH tank, and fermentation tank, respectively. In addition, the whole process requires 49,775.98 MJ h⁻¹ to maintain a proper temperature. Thus, data indicated that this process generated an energy surplus of 26,992.35 MJ h⁻¹. Most of the energy was demanded during the pretreatment stage. Specifically, 99% of the energy was associated to steam production at a T of 121 °C. Finally, the energy balance of the process showed an energy surplus of 35% considering the quantity of bioethanol produced minus the energy required by the process. Taking into account the fundamental stages studied in the present work and from an energetic point of view, the process presented herein could be labeled as sustainable. Thus, it may be successfully implemented at the industrial level.

3.4. X-ray analysis (Crystallinity)

Crystallinity significantly affects enzymatic hydrolysis efficiency. This parameter was determined using X ray diffraction (Morais et al., 2016). Fig. 4 shows X-ray spectra of SB exposed to different treatments. Characteristic peaks associated to cellulose I structure (16.1° and 22.7°) are also shown (Ávila-Lara et al., 2015; Montiel et al., 2016). Results

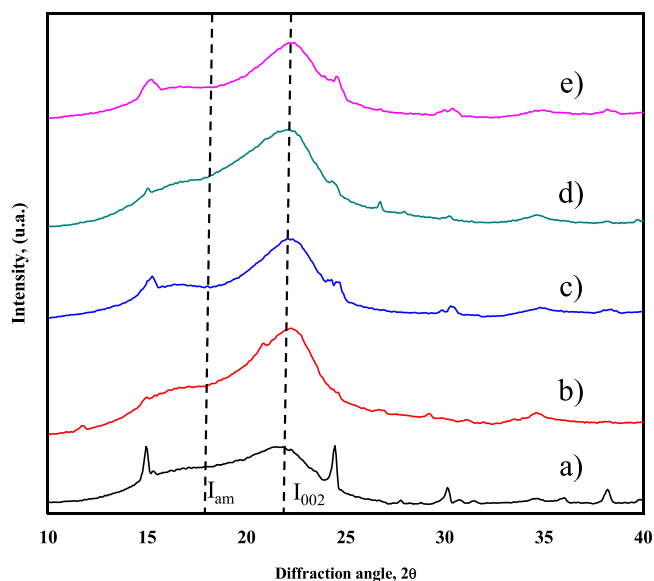


Fig. 4. X-ray spectra of SB after each process stage: a) raw material; b) acid pretreatment; c) alkali pretreatment; d) EH of SB after acid pretreatment; e) EH of SB after acid pretreatment.

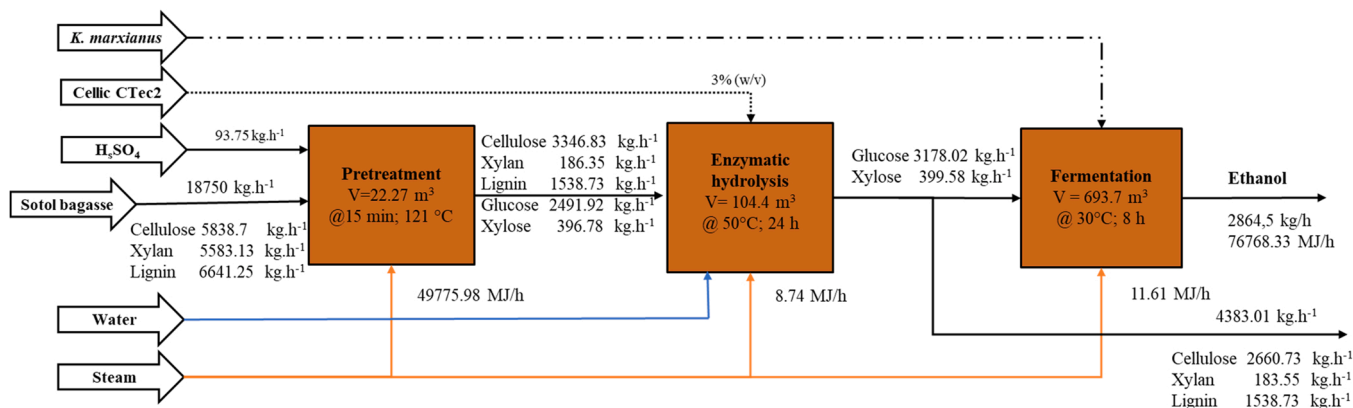


Fig. 3. Process block diagram for SB transformation: a) Pretreatment tank, b) Enzymatic hydrolysis tank, c) Fermentation tank.

indicated that untreated and acid pretreated biomasses displayed crystallinity indexes (*CrI*) of 6.6% and 30.89%, respectively. This increase in *CrI* was attributed to the removal of amorphous cellulose, hemicellulose, and lignin during the acidic pretreatment. After enzymatic hydrolysis, *CrI* was 21.05%. In this case, *CrI* decrease can be associated to crystalline cellulose hydrolysis and lignin removal after EH (Molina-Guerrero et al., 2018). *CrI* of biomass pretreated with alkali displayed a value of 33.3%, which was higher than that obtained for SB without pretreatment. Herein, a higher *CrI* also indicated reduced amorphous cellulose, hemicellulose, and lignin content. In addition, the *CrI* of biomass pretreated with alkali was higher than the one observed for acid pretreated biomass. This difference resulted from lignin and hemicellulose removal (Morais et al., 2016). According to these data, alkaline pretreatment was able to remove higher amounts of amorphous cellulose than acidic pretreatment. As previously reported in Aguirre-Fierro et al. (2020), an increase in *CrI* can be associated to the increase of cellulose content in the pretreated biomass. Moreover, after EH, *CrI* was 31.28%. This value was much higher than that obtained after EH of acid pretreated SB.

CrI is associated to cellulose and lignin content in biomass. Cellulose content in the raw material, biomass after basic pretreatment, and biomass after acidic pretreatment displayed values of (g/kg) 311.4, 474.7, and 542.2, respectively. Thus, SB with no pretreatment presented a low cellulose content and low crystallinity index (see Table 6). However, in both pretreatments (basic and acid) the cellulose content and *CrI* increased. In these results, the crystallinity index of alkaline pretreated biomass (31.28%) was higher as compared to that pretreated with acid (30.89%). These data may indicate that the alkaline pretreatment resulted in a higher exposure of cellulose fibers than acidic pretreatment.

CrI and lignin content are also related. For example, SB with no pretreatment displayed a high lignin content and a low *CrI*. However, *CrI* increases as lignin was removed during pretreatments. For example, the lignin content after basic pretreatment was lower as compared to that after acidic pretreatment. In addition, *CrI* was higher in the basic treated biomass as a result of a higher lignin removal (Morais et al., 2016).

Table 6 presents the results for crystallite size in the 002 plane and the crystallinity index for samples obtained in the present investigation. Data indicated that SB exhibited crystallite sizes between 2.59 and 3.9 nm. Crystal size in raw SB was of 3.9 nm, while that in acid pretreated SB was of 2.59 nm. In addition, crystallite size was 2.65 nm after EH. This size reduction may be attributed to the partial destruction of crystalline cellulose after SB pretreatment.

XRF analysis was performed to determine the content of SiO₂ in the biomass after pretreatment and hydrolysis. SiO₂ represents a plant defense against abiotic (e.g., heavy metal toxicity and salinity) and biotic (e.g., fungi and insects) stresses. Different operative complications reported in paper pulp plants or during wastewater treatment have been associated with the presence of SiO₂ precipitates, which significantly affect control systems during biorefinery processes (Le et al., 2015). Our data indicated that the content of silica was 2.447%, 4.352%, and 11.585% for SB without pretreatment, SB with acid pretreatment, and hydrolyzed SB, respectively. As expected, SiO₂ was not detected in fibers of biomass exposed to alkali pretreatment. Le et al. (2015) reported that the spontaneous solubilization of silica in water was highly dependent on pH and temperature (pH over 9). The influence of pH and temperature on silica solubility is extremely important since many industrial biorefinery processes involve different steps that are performed at

relatively low pHs (e.g. hydrolysis, dehydration, and rehydration) and specific temperatures (Le et al., 2015). Our results indicated a silica content in SB similar to that observed in wheat straw (2.53%) (Molina-Guerrero et al., 2018). Higher values for SiO₂ content in acid treated biomass may be attributed to a decrease in amorphous cellulose content.

3.5. SEM analysis

Fig. 5 depicts the micrographs of raw material and SB after chemical pretreatment and enzymatic hydrolysis. In this Figure, different morphological changes are observed. Fig. 5a corresponds to SB without pretreatment. As this image reveals, fibers presented a defined structure and an intact epidermis covering the SB skeletal structure. In Fig. 5b, the SB exposed to diluted sulfuric acid pretreatment (AP1) showed a structure with no presence of epidermis and an exposed skeletal structure (cellulose). Finally, Fig. 5c presents the micrographs of SB after hydrolysis. In this case, fibers displayed a completely amorphous configuration, indicating structure degradation. Fig. 5d shows morphological SB changes after alkaline pretreatment. In this case, fiber internal structures were exposed, uncovering cellulose and hemicellulose components. For this reason, hydrolysis performance improved. Fig. 5e presents the skeletal structure of SB fibers, where significant fiber damage is observed.

3.6. Total Attenuated Reflection (ATR) (Infra-Red)

ATR band assignments were performed according to literature specialized in the analysis of cellulose, hemicellulose, and lignin biomolecules. The characteristic ATR spectra (Fig. A2) are shown in the Supplementary information. The cellulose bands are associated to CH₂ (1319 cm⁻¹), ring vibrational stretching C-O-C (1157 cm⁻¹), aromatic C-H deformation (1022 cm⁻¹) and stretching due to β-linkage in cellulose (887 cm⁻¹) (Cui et al., 2012; Kirtania et al., 2014). The ATR band at 1022 cm⁻¹ displayed strong signals characteristic of a high cellulose content. This band, which was present in every sample, was correlated with cellulose and is probably associated with β (1,3)-polysaccharides (Molina-Guerrero et al., 2018).

The ATR bands associated with hemicellulose were found at 1731 and 1226 cm⁻¹. The ATR band at 1731 cm⁻¹ corresponded to an ester carbonyl group (C=O) and displayed a typical band associated with hemicellulose (Kirtania et al., 2014; Kristensen et al., 2008; Martínez-Herrera et al., 2021).

The ATR lignin bands were found at 1592 and 1504 cm⁻¹. These signals corresponded to quadrant ring stretching (aromatic lignin) and semicircle ring stretching (aromatic lignin), respectively (Kristensen et al., 2008). The bands at 3413 cm⁻¹ were related to the -OH groups present in different components including absorbed water in cellulose, hemicellulose, lignin, and carboxylic acids (Brígida et al., 2010; Cui et al., 2012; Ibrahim et al., 2011; Kristensen et al., 2008). Finally, Kristensen et al. (2008) ascribed the 2956 and 2906 cm⁻¹ bands to waxes associated with methyl (-CH₃) and methylene (-CH₂) groups (Kristensen et al., 2008; Martínez-Herrera et al., 2021).

4. Conclusion

In the present investigation we developed an integrative process for ethanol (2G) production using sotol bagasse biomass, which represents a

Table 6
Crystallinity index, crystal size, and SiO₂ content in biomass fibers before and after pretreatments.

Issue	Raw material	Acid pretreatment	EH of acid pretreated biomass	Alkali pretreatment	EH of alkali pretreated biomass
Crystallinity index [%]	6.62	30.89	21.05	33.3	31.28
Crystal size [nm]	3.9	2.59	2.65	2.99	3.42
SiO ₂ [%]	2.447	4.352	11.585	N.D.	N.D.

N.D. No detected.

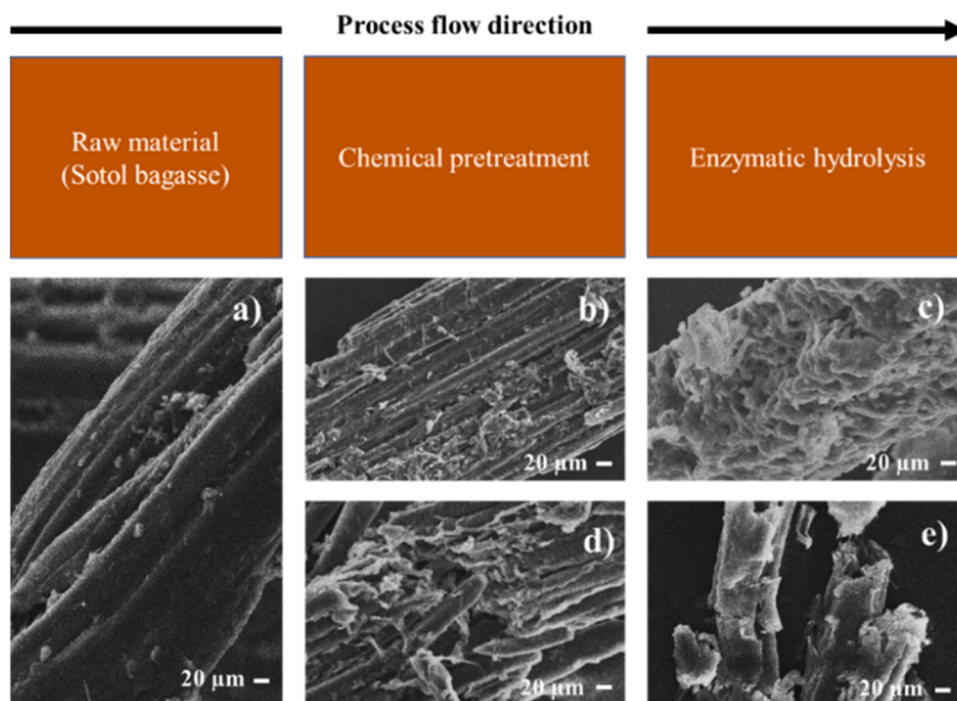


Fig. 5. SEM micrographs: a) raw material; b) acid pretreated SB; c) hydrolyzed SB after acid pretreatment; d) alkali pretreated SB; and e) hydrolyzed SB after alkali pretreatment.

novel carbon source produced in Mexico. For this purpose, we performed biomass characterization and developed the biofuel production process. Our data indicated that this process adheres to the principles of green chemistry since a significant amount of energy was obtained. This amount was significantly higher than $49,775.98 \text{ MJ h}^{-1}$, which corresponds to the energy required to produce ($76,768.33 \text{ MJ h}^{-1}$) ethanol. Thus, from an energetic point of view, bioethanol production using SB is a feasible process. Our polysaccharide SB content indicated a low performance during the scale up process. Thus, new strategies will be developed to improve performance of pretreatment and hydrolysis processes. In conclusion, SB showed a significant potential for the production of 2G ethanol. Furthermore, our proposed process will support the transition to a circular bioeconomy in Mexico.

CRediT authorship contribution statement

Jésica de Jesús Gonzalez-Chavez: Investigation, Writing – original draft. **Christian Arenas-Grimaldo:** Investigation, Writing – original draft. **Lorena Amaya-Delgado:** Writing – review & editing, Material resources, Instrumentation. **Edgar Vazquez-Núñez:** Writing – review & editing. **Juan Gabriel Segovia-Hernández:** Writing – review & editing, Funding acquisition, Resources, Methodology. **Santiago Suarez-Vázquez:** Writing – review & editing, Instrumentation. **Arquímedes Cruz-López:** Writing – review & editing, Instrumentation. **Samuel Pérez Vega:** Writing – review & editing, Instrumentation. **Iván Salmerón:** Writing – review & editing, Instrumentation. **Carlos E. Molina-Guerrero:** Conceptualization, Writing – review & editing, proposal writing and funding, Project administration. All the authors read and approved the submitted version of the manuscript.

Declaration of Competing Interest

The authors declare that they have no known competing financial interests or personal relationships that could have appeared to influence the work reported in this paper.

Acknowledgments

We acknowledge financial support from Universidad de Guanajuato DIQEB-Science and Engineering Division and Dirección de Apoyo a la Investigación y al Posgrado (Convocatoria Institucional de Investigación Científica 2021) project (054/2021) and project (015/2021). J. González-Chavez acknowledges financial support from CONACyT, Mexico (MSc scholarship 903184. We thank Doctor Guadalupe de la Rosa for manuscript editing.

Appendix A. Supporting information

Supplementary data associated with this article can be found in the online version at [doi:10.1016/j.indcrop.2022.114571](https://doi.org/10.1016/j.indcrop.2022.114571).

References

- Adney, B., Baker, J., 2008. Measurement of Cellulase Activities: Laboratory Analytical Procedure (LAP); Issue Date: 08/12/1996. <https://doi.org/NREL/TP-510-42628>.
- Aguirre-Fierro, A., Ruíz, H.A., Cerqueira, M.A., Ramos-González, R., Rodríguez-Jasso, R. M., Marques, S., Bogel-Lukasik, R., 2020. Sustainable approach of high-pressure agave bagasse pretreatment for ethanol production. *Renew. Energy* 155, 1347–1354. <https://doi.org/10.1016/j.renene.2020.04.055>.
- Amaya-Delgado, L., Herrera-López, E.J., Arrizon, J., Arellano-Plaza, M., Gschaedler, A., 2013. Performance evaluation of *Pichia kluyveri*, *Kluyveromyces marxianus* and *Saccharomyces cerevisiae* in industrial tequila fermentation. *World J. Micro Biot.* 29, 875–881. <https://doi.org/10.1007/s11274-012-1242-8>.
- Ávila-Lara, A.I., Camberos-Flores, J.N., Mendoza-Pérez, J.A., Messina-Fernández, S.R., Saldaña-Duran, C.E., Jimenez-Ruiz, E.L., Sánchez-Herrera, L.M., Pérez-Pimentá, J. A., 2015. Optimization of alkaline and dilute acid pretreatment of agave bagasse by response surface methodology. *Front. Bioeng. Biotechnol.* 3, 1–10. <https://doi.org/10.3389/fbioe.2015.00146>.
- Bajwa, D.S., Peterson, T., Sharma, N., Shojaeiarani, J., Bajwa, S.G., 2018. A review of densified solid biomass for energy production. *Renew. Sustain. Energy Rev.* <https://doi.org/10.1016/j.rser.2018.07.040>.
- Bell, W.H., Castetter, E.F., 1941. The utilization of yucca, sotol and beargrass by the aborigines in the American Southwest. University of New Mexico biological series, v. 5, no. 5, bulletin 372, Ethnobiological studies in the American Southwest, 7 5, 5. https://digitalrepository.unm.edu/unm_bulletin/33.
- Brígida, A.I.S., Calado, V.M.A., Gonçalves, L.R.B., Coelho, M.A.Z., 2010. Effect of chemical treatments on properties of green coconut fiber. *Carbohydr. Polym.* 79, 832–838. <https://doi.org/10.1016/j.carbpol.2009.10.005>.

- Cardona Alzate, C.A., Sánchez Toro, O.J., 2006. Energy consumption analysis of integrated flowsheets for production of fuel ethanol from lignocellulosic biomass. *Energy* 31, 2447–2459. <https://doi.org/10.1016/j.energy.2005.10.020>.
- Carrillo-Nieves, D., Rostro Alanís, M.J., de la Cruz Quiroz, R., Ruiz, H.A., Iqbal, H.M.N., Parra-Saldívar, R., 2019. Current status and future trends of bioethanol production from agro-industrial wastes in Mexico. *Renew. Sustain. Energy Rev.* <https://doi.org/10.1016/j.rser.2018.11.031>.
- Chundawat, S.P.S., Balan, V., Dale, B.E., 2008. High-throughput microplate technique for enzymatic hydrolysis of lignocellulosic biomass. *Biotechnol. Bioeng.* 99, 1281–1294. <https://doi.org/10.1002/bit.21805>.
- Cui, L., Liu, Z., Si, C., Hui, L., Kang, N., Zhao, T., 2012. Influence of steam explosion pretreatment on the composition and structure of wheat straw. *BioResources* 7, 4202–4213. <https://doi.org/10.15376/biores.7.3.4202-4213>.
- Delgado, R., Castro, A.J., Vázquez, M., 2009. A kinetic assessment of the enzymatic hydrolysis of potato (*Solanum tuberosum*). *LWT - Food Sci. Technol.* 42, 797–804. <https://doi.org/10.1016/j.lwt.2008.11.001>.
- Esposito, D., Antonietti, M., 2015. Redefining biorefinery: the search for unconventional building blocks for materials. *Chem. Soc. Rev.* 44, 5821–5835. <https://doi.org/10.1039/c4cs00368c>.
- Ferraresi de Araujo, J.G., Niño-Castillo, I.N., 2021. Vinasse: current concepts, challenges and opportunities for the sustainability. *ECORFAN J. -Repub. Nicar.* 7, 1–9. <https://doi.org/10.35429/EJRN.2021.13.7.1>.
- Flores-Cosío, G., Arellano-Plaza, M., Gschaedler, A., Amaya-Delgado, L., 2018. Physiological response to furan derivatives stress by *Kluyveromyces marxianus* SLP1 in ethanol production. *Rev. Mex. Ing. Quím.* 17, 189–202. <https://doi.org/10.24275/uam/izt/dcbi/revmexingquim/2018v17n1/Flores>.
- Flores-Gallegos, A.C., Cruz-Requena, M., Castillo-Reyes, F., Rutiaga-Quiñones, M., Sepulveda-Torre, L., Paredes-Ortiz, A., Soto, O., Rodríguez-Herrera, R., 2019. Sotol, an Alcoholic Beverage With Rising Importance in the Worldwide Commerce, Alcoholic Beverages. Elsevier Inc. <https://doi.org/10.1016/B978-0-12-815269-0.00005-2>.
- Ibrahim, M.M., El-Zawawy, W.K., Abdel-Fattah, Y.R., Soliman, N.A., Agblevor, F.A., 2011. Comparison of alkaline pulping with steam explosion for glucose production from rice straw. *Carbohydr. Polym.* 83, 720–726. <https://doi.org/10.1016/j.carbpol.2010.08.046>.
- Igathinathane, C., Sanderson, M., 2018. Biofuel Feedstock: Challenges and Opportunities, in: *Green Chem Sus Biofuel Prod.* <https://doi.org/10.1201/b22351-2>.
- Karim, A., Gerliani, N., Aider, M., 2020. *Kluyveromyces marxianus*: an emerging yeast cell factory for applications in food and biotechnology. *Int. J. Food Microbiol.* 333, 108818. <https://doi.org/10.1016/j.ijfoodmicro.2020.108818>.
- Karlsson, H., Pål, B., Per-Anders, H., Ahlgren, S., 2014. Ethanol production in biorefineries using lignocellulosic feedstock - GHG performance, energy balance and implications of life cycle calculation methodology. *J. Clean. Prod.* 83, 420–427. <https://doi.org/10.1016/j.jclepro.2014.07.029>.
- Kirtania, K., Tanner, J., Kabir, K.B., Rajendran, S., Bhattacharya, S., 2014. In situ synchrotron IR study relating temperature and heating rate to surface functional group changes in biomass. *Bioresour. Technol.* 151, 36–42. <https://doi.org/10.1016/j.biortech.2013.10.034>.
- Kristensen, J.B., Thygesen, L.G., Felby, C., Jørgensen, H., Elder, T., 2008. Cell-wall structural changes in wheat straw pretreated for bioethanol production. *Biotechnol. Biofuel* 1, 1–9. <https://doi.org/10.1186/1754-6834-1-5>.
- Láinez, M., Ruiz, H.A., Arellano-Plaza, M., Martínez-Hernández, S., 2019. Bioethanol production from enzymatic hydrolysates of *Agave salmiana* leaves comparing *S. cerevisiae* and *K. marxianus*. *Renew. Energy* 138, 1127–1133. <https://doi.org/10.1016/j.renene.2019.02.058>.
- Le, D.M., Sørensen, H.R., Knudsen, N.O., Meyer, A.S., 2015. Implications of silica on biorefineries – interactions with organic material and mineral elements in grasses. *Biofuel Bioprod. Bioref.* 9, 109–121. <https://doi.org/10.1002/bbb.1511>.
- Leonel, L.V., Arruda, P.V., Chandel, A.K., Felipe, M.G.A., Sene, L., Arruda, P.V., Chandel, A.K., Felipe, M.G.A., Sene, L., 2021. *Kluyveromyces marxianus*: a potential biocatalyst of renewable chemicals and lignocellulosic ethanol production. *Crit. Rev. Biotechnol.* 0, 1–39. <https://doi.org/10.1080/07388551.2021.1917505>.
- López-Ortega, M., Guadalupe, Y., Junqueira, T., Sampaio, I., Bonomi, A., Sánchez, A., 2021. Sustainability analysis of bioethanol production in Mexico by a retrofitted sugarcane industry based on the Brazilian expertise. *Energy* 232. <https://doi.org/10.1016/j.energy.2021.121056>.
- Luciano Silveira, M.H., Morais, A.R.C., da Costa Lopes, A.M., Nayara Oleksyszyn, D., Bogel-Lukasik, R., Andreus, J., Pereira Ramos, L., 2015. Current pretreatment technologies for the development of cellulose ethanol and biorefineries. *Chem. Sustain. Energy Mater.* 8, 3366–3390. <https://doi.org/10.1002/cssc.201500282>.
- Manzanares, P., 2020. The role of biorefining research in the development of a modern bioeconomy. *Acta Innov.* 37, 47–56. (<https://orcid.org/0000-0001-7735-4796>).
- Martínez-Herrera, R.E., Alemán-Huerta, M.E., Flores-Rodríguez, P., Almaguer-Cantú, V., Valencia-Vázquez, R., Rosas-Flores, W., Medrano-Roldán, H., Ochoa-Martínez, L.A., Rutiaga-Quiñones, O.M., 2021. Utilization of *Agave durangensis* leaves by *Bacillus cereus* 4N for polyhydroxybutyrate (PHB) biosynthesis. *Int. J. Biol. Macromol.* 175, 199–208. <https://doi.org/10.1016/j.ijbiomac.2021.01.167>.
- Merediane Kochepka, D., Pastre Dill, L., Henrique Fockink, D., Łukasik, R.M., 2020. Contribution to the production and use of biomass-derived solvents – a review. *Acta Innov.* 29–56. <https://doi.org/10.32933/ActaInnovations.35.3>.
- Miller, G.L., 1959. Use of dinitrosalicylic acid reagent for determination of reducing sugar. *Anal. Chem.* 31, 426–428. <https://doi.org/10.1021/ac60147a030>.
- Molina, C., Sánchez, A., Serafin-Muñoz, A., Folch-Mallol, J., 2014. Optimization of enzymatic saccharification of wheat straw in a micro-scale system by response surface methodology. *Rev. Mex. Ing. Quím.* 13, 765–778. <https://www.redalyc.org/pdf/620/62035738010.pdf>.
- Molina Guerrero, C.E., Valdez-Vazquez, I., Macías Mora, M., León Pérez, K., Ibarra Sánchez, J., Alcántara Ávila, J.R., 2021. Development of a bidimensional analysis approach for n – butanol and electricity production in apple pomace biorefineries in a Mexican context. *Biomass Conv. Bioref.* 1–10. <https://doi.org/10.1007/s13399-021-01472-3>.
- Molina-Guerrero, C.E., de la Rosa-Álvarez, M.G., Castillo-Michel, H., Sánchez, A., García-Castañeda, C., Hernández-Rayas, A., Valdez-Vazquez, I., Suarez-Vázquez, S., 2018. Physicochemical characterization of wheat straw during a continuous pretreatment process. *Chem. Eng. Technol.* 41, 1350–1358. <https://doi.org/10.1002/ceat.201800107>.
- Molina-Guerrero, C.E., Sanchez, A., Vázquez-Núñez, E., 2020. Energy potential of agricultural residues generated in Mexico and their use for butanol and electricity production under a biorefinery configuration. *Environ. Sci. Pollut. R* 27, 28607–28622. <https://doi.org/10.1007/s11356-020-08430-y>.
- Moncada, J., Aristizábal, V., Cardona, C.A., 2016. Design strategies for sustainable biorefineries. *Biochem. Eng. J* 116, 122–134. <https://doi.org/10.1016/j.bej.2016.06.009>.
- Montiel, C., Hernández-meléndez, O., Vivaldo-lima, E., 2016. Enhanced bioethanol production from blue agave bagasse in a combined extrusion – saccharification process. *BioEnergy Res.* 9, 1005–1014. <https://doi.org/10.1007/s12155-016-9747-x>.
- Morais, A.R.C., Pinto, J.V., Nunes, D., Roseiro, L.B., Conceição, M., Fortunato, E., Bogel-Lukasik, R., 2016. Imidazole prospect solvent for lignocellulosic biomass fractionation and delignification. *Sustain. Chem. Eng.* <https://doi.org/10.1021/acsuscchemeng.5b01600>.
- Morales, M., Arvesen, A., Cherubini, F., 2021. Integrated process simulation for bioethanol production: effects of varying lignocellulosic feedstocks on technical performance. *Bioresour. Technol.* 328, 124833. <https://doi.org/10.1016/j.biortech.2021.124833>.
- Nagappan, S., Nakkeeran, E., 2020. Biorefinery: a concept for Co-producing biofuel with value-added products. *Environ. Chem. Sustain.* World 23–52. https://doi.org/10.1007/978-3-030-38196-7_2.
- Nom-159-Scfi, 2004. NOM-159-SCFI-2004. Diario Oficial de la Federación. <http://wwwordenjuridico.gob.mx/Documentos/Federal/wo45110.pdf>. (Accessed 3 January 2022).
- Ortiz-Méndez, O.H., Morales-Martínez, T.K., Ríos-González, L.J., Rodríguez-de la Garza, J.A., Quintero, J., Aroca, G., 2017. Bioethanol production from *Agave lechuguilla* biomass pretreated by autohydrolysis. *Rev. Mex. Ing. Quím.* 16, 467–476.
- Oseguera, I., Guillermo, V., Rodríguez, M., Omar, F., Muñoz, B., Gabriel, J., Hernández, Segovia, Hernández, Salvador, 2018. Multiplicities in dividing wall distillation columns in the purification of bioethanol: energy considerations. *Clean Technol. Environ.* 20, 1631–1637. <https://doi.org/10.1007/s10098-017-1415-0>.
- Perez-Pimienta, J.A., Lopez-Ortega, M.G., Varanasi, P., Stavila, V., Cheng, G., Singh, S., Simmons, B.A., 2013. Comparison of the impact of ionic liquid pretreatment on recalcitrance of agave bagasse and switchgrass. *Bioresour. Technol.* 127, 18–24. <https://doi.org/10.1016/j.biortech.2012.09.124>.
- Pino, M.S., Rodríguez-Jasso, R.M., Michelin, M., Ruiz, H.A., 2019. Enhancement and modeling of enzymatic hydrolysis on cellulose from agave bagasse hydrothermally pretreated in a horizontal bioreactor. *Carbohydr. Polym.* 211, 349–359. <https://doi.org/10.1016/j.carbpol.2019.01.111>.
- Ruiz, H.A., Galbe, M., Garrote, G., Ramirez-Gutierrez, D.M., Ximenes, E., Sun, S.-N., Lachos-Perez, D., Rodríguez-Jasso, R.M., Sun, R.-C., Yang, B., Ladisch, M.R., 2021. Severity factor kinetic model as a strategic parameter of hydrothermal processing (steam explosion and liquid hot water) for biomass fractionation under biorefinery concept. *Bioresour. Technol.* 342, 125961. <https://doi.org/10.1016/j.biortech.2021.125961>.
- Sanchez, A., Sevilla-Guitrón, V., Magaña, G., Gutierrez, L., 2013. Parametric analysis of total costs and energy efficiency of 2G enzymatic ethanol production. *Fuel* 113, 165–179. <https://doi.org/10.1016/j.fuel.2013.05.034>.
- Sandoval-Núñez, D., Arellano-Plaza, M., Gschaedler, A., Arrizon, J., Amaya-Delgado, L., 2017. A comparative study of lignocellulosic ethanol productivities by *Kluyveromyces marxianus* and *Saccharomyces cerevisiae*. *Clean Technol. Environ.* <https://doi.org/10.1007/s10098-017-1470-6>.
- Saucedo-Luna, J., Castro-Montoya, A.J., Martínez-Pacheco, M.M., Sosa-Aguirre, C.R., Campos-García, J., 2011. Efficient chemical and enzymatic saccharification of the lignocellulosic residue from Agave tequilana bagasse to produce ethanol by *Pichia caribbica*. *J. Ind. Microbiol. Biotechnol.* 38, 725–732. <https://doi.org/10.1007/s10295-010-0853-z>.
- Seader, J., Henley, E., 2011. *Separation Process Principles*, third ed. John Wiley & Sons, Inc, New Jersey.
- Segal, L., Creely, J.J., Martin, A.E., Conrad, C.M., 1959. An empirical method for estimating the degree of crystallinity of native cellulose using the X-Ray diffractometer. *Text. Res. J.* 29, 786–794. <https://doi.org/10.1177/004051755902901003>.
- Sluiter, A., Hames, B., Ruiz, R., Scarlata, C., Sluiter, J., Templeton, D., Crocker, D., 2011. Determination of Structural Carbohydrates and Lignin in Biomass Technical Report NREL/TP-510-42618. Laboratory Analytical Procedure (LAP). <https://doi.org/NREL/TP-510-42618>.
- Torres-Ortega, C.E., Ramírez-Márquez, C., Sánchez-Ramírez, E., Quiroz-Ramírez, J.J., Segovia-Hernández, J.G., Rong, B., 2018. Effects of intensification on process features and control properties of lignocellulosic bioethanol separation and dehydration systems. *Chem. Eng. Process.: Process Intensif.* 128, 188–198. <https://doi.org/10.1016/j.cep.2018.04.031>.
- US Department of Energy, 2016. Energy Efficiency and Renewable Energy. Strategic Plan for a Thriving and Sustainable Bioeconomy. 48 p. <https://www.energy.gov/sites/pro>

d/files/2016/12/f34/beto_strategic_plan_december_2016_0.pdf. (Accessed 3 January 2022).

Wild, M., Visser, L., 2018. Biomass pre-treatment for bioenergy. IEA Bioenergy.

Zavala-Díaz de la Serna, F., Contreras-López, R., Lerma-Torres, L.P., Ruiz-Terán, F., Rocha-Gutierrez, B., Pérez-Vega, S., Elias-Ogaz, L.R., Salmerón, I., 2020.

Understanding the biosynthetic changes that give origin to the distinctive flavor of sotol: microbial identification and analysis of the volatile metabolites profiles during sotol (*Dasyliirion* sp.) must fermentation. *Biomolecules* 10, 1063. <https://doi.org/10.3390/biom10071063>.